

β -Detected Nuclear Magnetic Resonance at ISAC

(G.D. Morris^a, R.F. Kieft^{a,b,c}, ^aTRIUMF, ^bCIAR and ^cUBC)

We are developing a beta-detected nuclear magnetic resonance (β -NMR) facility for studying materials and phenomena of interest in condensed matter physics. The initial spectrometer, designed for experiments in high longitudinal magnetic field, is virtually complete. Development of DAQ software to enable various experiments continues as we begin the experimental program.

Introduction

Nuclear magnetic resonance is a powerful experimental technique that yields information about the electronic, chemical and magnetic environment and dynamics present in materials. In the nuclear-detected techniques of β -NMR and μ SR radioactive probes are implanted and information about the local environment is revealed through the anisotropic distribution of the outgoing decay products. Specific and often unique features of these various resonance techniques make each well suited to certain experiments. β -NMR at ISAC is being developed to take advantage of the high flux of low energy spin polarized radioisotopes, particularly for experiments on ultra thin samples and over a wide range of magnetic fields and temperatures.

The scientific motivation as well as the layout and functions of the polarizer and high field spectrometer have been described in detail previously [1, 2].

Polarization

A key milestone achieved this past year has been the polarization of ^8Li atoms with an in-flight optical pumping technique. The largest polarization achieved thus far has been about 40%. However, the installation of a ring laser in 2001 is expected to result in a larger and more stable nuclear polarization. Developments in the polarizer section are described in detail elsewhere in this Annual Report by C.D.P. Levy *et al.*

Beam spot imaging

In order to precisely focus and steer the radioactive ion beam spot onto small samples we have developed a CCD camera system to image the light produced when the ion beam is stopped in a piece of scintillator at the sample position. This system allows one to make adjustments to the electrostatic optical elements which define the position and shape of the beam spot in nearly real time.

This system is based on a 16-bit monochrome CCD camera (model MX516 manufactured by Starlight Xpress, UK) incorporating a cooled, low-noise CCD

sensor which allows long exposures to be made. A 50mm f/1.4 lens provides a narrow 7° field of view on the 500×290 pixel CCD. Peak sensitivity of the CCD occurs at 500-550 nm, close to the emission wavelength of several types of plastic and inorganic (UHV compatible) scintillation detectors.

The camera is mounted outside the UHV chamber but views the sample face almost along the beam axis through a UHV viewport and via a first surface mirror inside the UHV chamber which provides an approximately 90° bend in the optical path. The mirror is mounted on a hinge so it may be moved into position in front of the backward counter, slightly offset from the incoming ion beam.

For each ^8Li ion, energy is deposited in the scintillator in three ways. The initial beam energy is the smallest contribution, and the outgoing minimum-ionizing betas contribute about 100 keV on average. Most of the light will be generated by two very short-ranged α particles produced in the decay of an excited state of ^8Be , contributing about 1.6 MeV. Thus, the source of light within the scintillator is well correlated with the spatial distribution of implanted ions.

Exposures of about 30 s are sufficient to record the ^8Li beam spot with an ion flux of about 10^7 s^{-1} incident on 0.25 mm thick Bicron BC412 plastic scintillator. An example of the image of the beam spot is shown in Fig. 1. With longer exposures it is also possible to image the light produced by 100 nA beams of *stable* ions obtained from an off-line ion source.

Low energy implantation

Since the atoms in the ISAC production targets are initially thermal they are accelerated through a potential difference of 30 kV as they are injected into the beam line which transports them to an experiment. Such a low energy allows the use of electrostatic optics in the beam line and also makes it possible to vary the implantation energy by biasing the sample to a high voltage. The design of the spectrometer takes advantage of this to enable very low implantation energies and consequently very shallow implantation depths. The entire spectrometer including the superconducting solenoid, cryostat and all the electronics are mounted on a high voltage platform so that the ion energy at the sample surface may be varied from about 1 to 90 keV. The resulting mean implantation depth ranges from about 50–3000 Å. Conventional NMR does not have sufficient sensitivity to detect a signal from the small number of atoms in such a thin layer, especially in weak magnetic fields where the low Larmor frequency would result in a very small signal in an inductive pickup coil. Experiment 897 will use this low energy and low field capability to directly probe the magnetic field just

within the sample surface to make an absolute determination of the London penetration depth in superconductors in the Meissner state. Analogous μ SR experiments have been performed with low energy muons (LEM) at the Paul Scherrer Institute [3], however the muon event rates remain at least 4 to 5 orders of magnitude lower than rates we have demonstrated at ISAC. This year “soft landing” of ^8Li has been demonstrated down to 5 keV and should proceed to lower energies as tunes are developed. A long-awaited UHV-compatible replacement for the existing superconducting magnet in the high field spectrometer will be installed early in 2001. With the bakable magnet true UHV conditions will be reached so that low temperature experiments can be performed with kinetic energies down to about 1 keV. The electrode assembly which shapes the deceleration potential is presently being rebuilt in a more robust and more precisely aligned assembly.

RF control and DAQ

All of the electronics required to generate precise timing signals simultaneously with amplitude- and frequency-modulated RF power are now installed. A great deal of progress has been made in the software which configures and controls various types of experiments in real time.

Unlike conventional NMR, the nuclear-detected NMR techniques do not require a tuned high-Q RF coil for detecting the NMR signal. This allows the use of a broadband coil to generate the RF magnetic field and consequently one can sweep RF frequency over a wide range – 0-40 MHz in the present design – without any need to change the coil. With appropriate modulation of the RF power it should be possible to irradiate with several frequencies simultaneously.

Figure 2 shows the first resonance observed with the spectrometer in which ^8Li was stopped in a Pd foil in a magnetic field of 3 T at room temperature. During this run the beam was implanted continuously while the RF frequency was repeatedly ramped from 18.93 to 18.99 MHz in 100 Hz steps every 4 ms. Depolarization of the implanted spins occurs when the RF frequency reaches the Larmor frequency, so the resonance reflects the distribution of local magnetic field at the site of the ions. After the RF has swept over the resonance the decay asymmetry recovers as the unpolarized population of spins is gradually replaced with new, polarized ions. This mode is useful for quickly searching a range of frequencies in order to locate resonances. The width of the line in Pd was found to be about 2 kHz.

Another DAQ mode makes use of the ability to pulse the incoming beam with an electrostatic kicker and control the RF frequency and power with a pulse programmer, RF synthesizer and arbitrary function

generator. In Fig. 3 the flat line was obtained with the beam polarization off, yielding a baseline which is very useful for fitting a relaxation function. The top curve shows the beta decay asymmetry in the absence of any RF power, in which the (Korringa) relaxation is known to be caused by the interaction with conduction electrons in the metal. When RF power at the Larmor frequency is applied after the beam pulse, and kept on to the end of the histogram, a portion of the polarization is quickly destroyed. It appears that continuous RF causes depolarization. but only of those nuclei close to the centre of the resonance line, the remaining nuclei in the wings come into resonance more slowly, probably as those ions diffuse to sites where they are subject to smaller dipolar fields.

The ability to manipulate spins with sequences of complex RF pulses is essential to many planned NMR experiments. In Fig. 4 we show a sharp step in the Back-Front asymmetry when a short, amplitude-modulated RF pulse is applied on resonance after the beam was shut off. The two spectra shown - with longitudinal polarization in each orientation along the z-axis - were taken by alternating the handedness of the circularly polarized laser light throughout the run while routing events to the corresponding histograms. Plotting the amplitude of the resulting step in asymmetry as a function of RF pulse length (see Fig. 5) we see that the projection of the polarization along the z-axis follows a cosine dependence; spins are being flipped through 180° with a pulse of about 1 ms duration.

In summary, the first β -NMR spectrometer is virtually complete. We are currently working to optimize the polarization so that the experimental program can be carried out as efficiently as possible. Many features of the DAQ and control system are now working and more are being added. We are about to begin the first experiments on semiconductors and superconductors

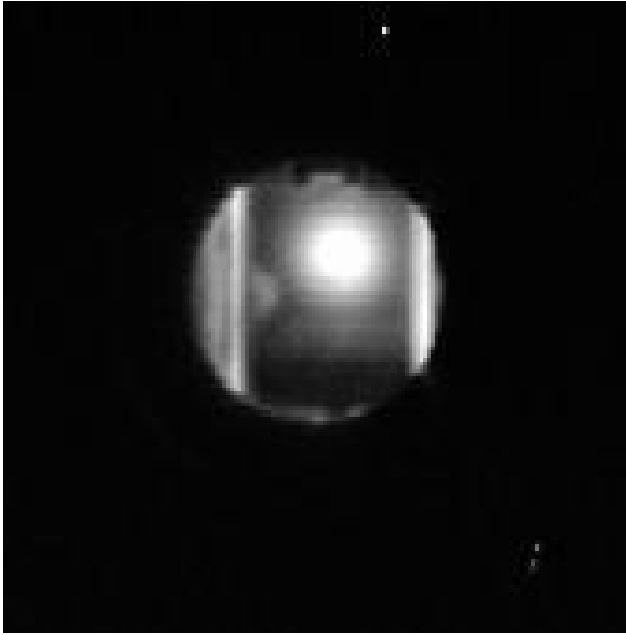


Fig. 1. An image of a slightly off-centre beam spot of ^8Li landing on a 8 mm wide piece of Bicron BC412 scintillator. Contrast has been adjusted to reveal the edges (bright vertical lines) of the scintillator and some of the cryostat parts; the FWHM of the spot is about 2 mm.

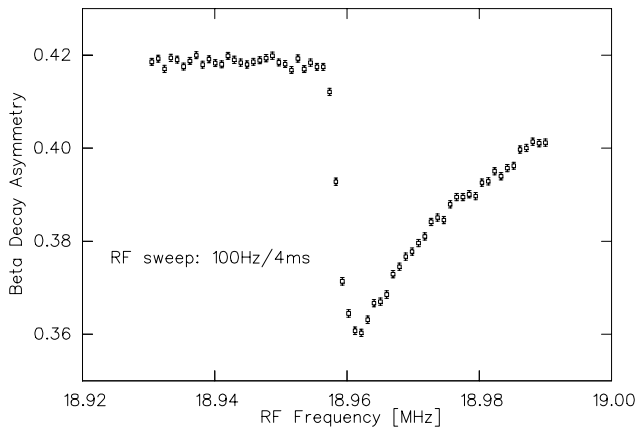


Fig. 2. First observation of resonant depolarization of ^8Li at ISAC. In this run the decay asymmetry was recorded while RF frequency was rapidly swept over the resonance in a constant magnetic field of 3 T.

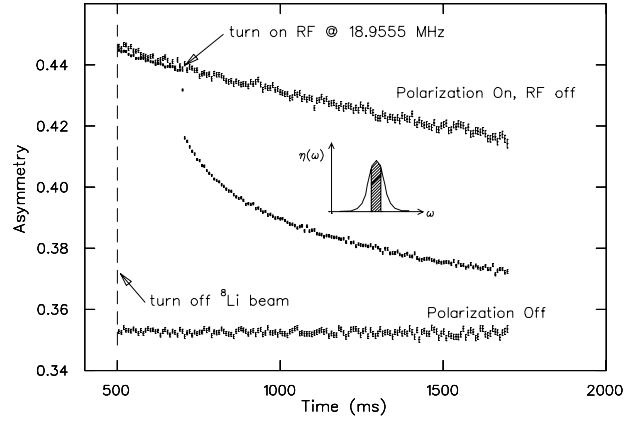


Fig. 3. Bottom curve: beta decay asymmetry without beam polarization; top; exponential spin relaxation without RF; centre: resonant depolarization with RF applied just after the ^8Li beam was switched off.

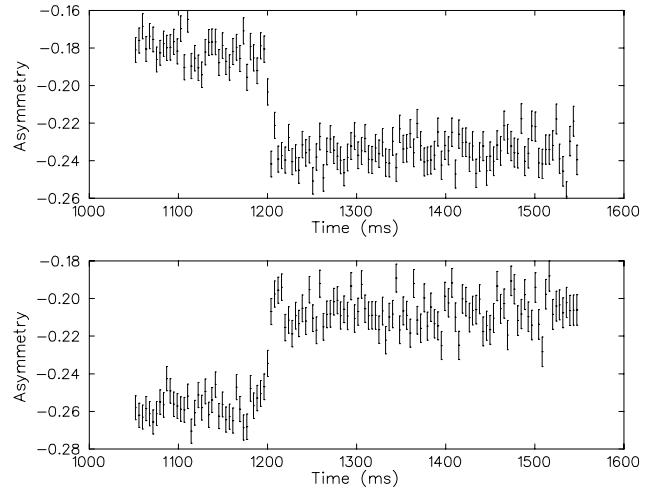


Fig. 4. Examples of time-differential spectra in which a short RF pulse was applied after the end of a pulse of beam. The step in decay asymmetry is due to precession of the spins in the RF magnetic field. Both orientations of initial polarization were acquired in the same run.

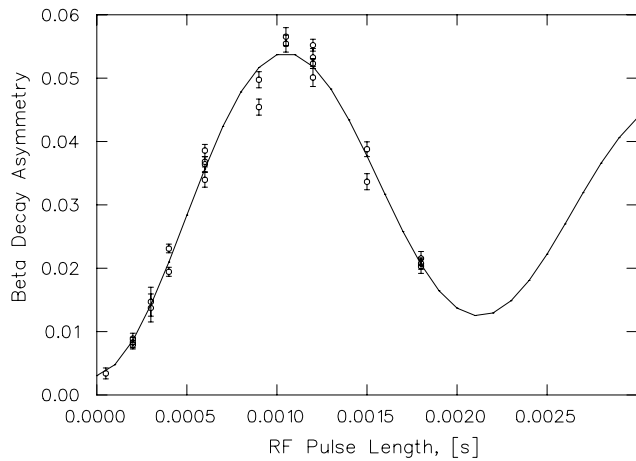


Fig. 5. Change in Back-Front asymmetry (the amplitude of the step in Fig. 4) as a function of RF pulse length. Asymmetry oscillates about the baseline, indicating that spins are being rotated coherently by the RF magnetic field.

References

- [1] R.F. Kiefl *et.al.*, *Physica B* 289-290 (2000), 640-647.
- [2] G.D. Morris, R.F. Kiefl, TRIUMF Annual Report Scientific Activities 1999, 116.
- [3] T.J. Jackson *et.al.*, *Phys. Rev. Lett.* 84 (2000) 4958.

Publications:

“Complementarity of low-energy spin polarized radioactive nuclei and muons”. R.F. Kiefl *et.al.*, *Physica B* 289-290 (2000), 640-647.

Presentations:

“ β -NMR at ISAC”, G.D. Morris, TRIUMF seminar, 7 Sept. 2000.

“Applications of β -NMR in materials science”, G.D. Morris, invited talk at the RIA Applications Workshop, Los Alamos Nat. Lab., 29-30 Oct. 2000.